Mission Energy Prediction for Unmanned Ground Vehicles Using Real-time Measurements and Prior Knowledge

Amir Sadrpour and Jionghua (Judy) Jin
Department of Industrial and Operations Engineering, University of Michigan, Ann Arbor, Michigan 48109
e-mail: sadrpour@umich.edu, jhjin@umich.edu
A. Galip Ulsoy
Department of Mechanical Engineering, University of Michigan, Ann Arbor, Michigan 48109
e-mail: ulsoy@umich.edu

Received 21 October 2012; accepted 8 February 2013

A typical unmanned ground vehicle (UGV) mission can be composed of various tasks and several alternative paths. Small UGVs are typically teleoperated and rely on electric rechargeable batteries for their operations. Since each battery has limited energy storage capacity, it is essential to predict the expected mission energy requirement during the mission execution and update this prediction adaptively via real-time performance measurements (e.g., vehicle power consumption and velocity). We propose and compare two methods in this paper. One is based on recursive least-squares estimation built upon a UGV longitudinal dynamics model. The other is based on Bayesian estimation when prior knowledge (e.g., road average grade and operator driving style) is available. The proposed Bayesian prediction can effectively combine prior knowledge with real-time performance measurements for adaptively updating the prediction of the mission energy requirement. Our experimental and simulation studies show that the Bayesian approach can yield more accurate predictions even with moderately imprecise prior knowledge.

1. INTRODUCTION

This paper considers the problem of mission energy prediction for battery-operated unmanned ground vehicles (UGVs) undertaking a specific mission, for example, a teleoperated UGV being used for local surveillance.

UGVs are entering the economic mainstream and are being used more extensively in military as well as commercial applications (Tilbury and Ulsoy, 2011). Unlike industrial robots, they are not yet very reliable. This is primarily due to the following factors:

1. The diversity and uncertainty of their operating environments. For example, the reliability of a UGV operated in a carpeted air-conditioned building can be expected to be much better than that of the same UGV operated in a sandy and hot desert environment.
2. The complex interactions between the UGV and its human operator. For example, teleoperated UGVs are difficult to operate, and an untrained operator may use the UGV in ways it has not been designed for.
3. New immature technologies being used in UGVs. For example, new sensors, signal processing, and artificial intelligence technologies used in UGVs may not operate well in all situations encountered.

Direct correspondence to: A. Sadrpour, e-mail: sadrpour@umich.edu.

The reliability problems associated with the current generation of UGVs have been discussed in detail in Carlson and Murphy (2003, 2005), Carlson et al. (2004), Kramer and Murphy (2006), Stancliff and Dolan (2005), and Sadrpour et al. (2011). One of the key factors that limit the utility of small teleoperated battery-powered UGVs is the available onboard energy. Typical mission durations are currently on the order of 1–2 h, while it is often desirable to carry out much longer missions (e.g., 8–10 h) between lengthy recharging stops. For a typical UGV, the primary source of energy consumption is the vehicle locomotion. For example, typical relative order-of-magnitude power requirements might be 100 W for propulsion, 10 W for computation, and 1 W for communication. Furthermore, the power requirement for propulsion can vary dramatically with road conditions (i.e., paved vs. unpaved), road grade (i.e., uphill vs. downhill), as well as driving styles (i.e., velocity profiles).

To address these challenges, the goal of this research is to develop a method for UGV mission energy prediction to provide the best possible estimate of available end-of-mission energy. As an example, we attempt to predict the energy requirement for conducting a surveillance mission. A typical surveillance mission consists of various tasks and several alternative paths that a UGV can select. Since each battery has limited energy storage capacity, it is essential to predict the expected energy requirements for alternative paths and to inform the operator.

A simple naive approach for the prediction of the mission energy requirement, which does not require a model, is to use the average current draw from the battery along with an estimate of the remaining duration of the mission. Assuming that the battery voltage remains almost constant throughout a mission, the product of battery average current draw, voltage, and the remaining duration of the mission provides a simple estimate of the expected energy requirement of the mission. The naive approach has some major limitations, such as poor predictions when UGVs move under quite different road conditions.

Consider a surveillance mission with the goal of traveling from a base to a destination where the UGV needs to traverse two road segments to accomplish the mission. The first road segment is downhill with an asphalt road surface, and the second road segment is on average flat and is a grass surface. Without knowledge of the terrains that the vehicle will face, one can assume that at any point in the mission, the future power requirement will be similar to that of the past (e.g., the naive approach). Thus, if we can collect and monitor the instantaneous power consumption of the vehicle, the average power consumption from past measurements can be used to predict future power consumption. When the vehicle traverses the first road segment (i.e., downhill/asphalt), the power consumption is substantially less than when it traverses the second road segment (flat/grass). Consequently, if the average power measurements from the first road segment were used to predict future energy requirements, the resulting predictions would considerably underestimate the true energy requirement of the mission. Our goal is to improve the predictions by integrating the available prior knowledge of road segment terrains with real-time sensory measurements.

We propose and compare two methods for predicting the energy requirement during the execution of a typical UGV mission based on the vehicle longitudinal dynamics: (i) a prediction method based on recursive least squares (RLS) estimation when there is no prior knowledge of the mission, and (ii) a Bayesian prediction method when the prior knowledge is obtainable. Although both methods utilize real-time measurements of UGV velocity and actual power consumption for updating the energy prediction, the Bayesian approach, which can consider prior knowledge of future tasks, is shown to achieve more accurate predictions compared to the first method, particularly in the initial stages of a mission.

The rest of the paper is organized as follows: Section 2 provides an overview of the literature in the area of UGV reliability to put into context the contributions of this research. Section 3 presents an overview of the proposed methodology. Sections 4 and 5 describe in detail the RLS estimation and the Bayesian approaches, respectively. Section 6 presents the experimental and simulation scenarios that illustrate the advantages of the proposed Bayesian approach. Concluding remarks are given in the final section.

2. LITERATURE REVIEW

Past endurance tests on small UGVs have shown that some operational failures can be prevented by real-time monitoring of key performance measures (Kramer and Murphy, 2006). Prognostics and health monitoring is an approach that permits the reliability of a system to be evaluated under actual operating conditions, and it has been discussed in Vichare et al. (2007), Lu (2001), Gorjian et al. (2009), and Lu, and Kolarik (2001). The limitation of such methods is that they have not incorporated mission prior knowledge, such as the duration of tasks, the nature and difficulty of the tasks ahead, or the operating style of the users, in their reliability assessments. In this paper, we consider mission prior knowledge and demonstrate its importance for more accurate energy requirement predictions.

Most UGVs use rechargeable batteries for their operations. One approach to predict the battery end of a cycle is to consider the history of its discharge rate. For instance, particle filters have been used to predict the battery end of a cycle (Saha et al. 2007; Saha et al. 2009, Saha and Goebel, 2008). However, the above prediction methods only use real-time data to determine the prediction of the battery end of a cycle. Consequently, ignorance of the intensity of the tasks ahead may lead to an over- or underestimation of the battery end of the cycle. More recently, particle filters have been used to predict the battery end of the cycle for unmanned aerial vehicles (UAVs) (Saha et al. 2011), in which the mission load profile obtained through offline experimentation is used to further improve the prediction of particle filters. However, since the environment with which the UAV interacts is not directly modeled, some inevitable changes in the actual mission profile, such as an increase in the duration of tasks, is difficult to incorporate in the prediction.

The ultimate goal of predicting energy requirements is to determine the probability of successful completion of a mission prior to exhausting the vehicle's stored energy. Power models for motion, sonar sensing, and control of mobile robots based on offline experimental results for the purpose of task planning and energy conservation are presented in Mei et al. (2004, 2005) and Dressler and Fuchs (2005). The models can be used in real-time if they have been calibrated prior to the mission. The limitations are that the

model parameters may vary from one robot to another and from one mission to the next and even within one mission depending on the intensity of tasks. Power prediction in automotive applications is typically based on standard drive cycles in conjunction with a vehicle longitudinal dynamics model (Ulsoy et al. 2012). Gondor and co-workers (2007) used GPS to collect driving cycle data from drivers of Plug-In Hybrid Electric cars. An approach for predicting the residual range of an electric vehicle (EV) is proposed in Ceraolo and Pede (2001). This approach considers the history of charge, the current driving conditions, and different driving styles to estimate the vehicle residual range, which is effective if the remaining period of the mission has the same characteristics as before. This assumption can be justified for automobiles since the road grades and conditions do not vary drastically. For UGV operations, however, the road condition as well as the road grade may vary significantly from one road segment to another. Additionally, for UGVs, more accurate prediction of energy is critical due to the much smaller quantity of stored energy compared to EVs. Conservative energy predictions can reduce the already limited operational capabilities of UGVs.

To overcome the limitations of current methods, we propose a new approach for predicting small UGV mission energy in the presence or absence of mission prior knowledge. In the absence of prior knowledge, the RLS estimation motivated by the vehicle longitudinal dynamics is used. In the presence of prior knowledge, a Bayesian prediction approach is used that integrates the prior knowledge with real-time measurements for improved predictions. The expected prior knowledge consists of qualitative information about the road condition and road grade, which can reasonably be expected to be known prior to a mission. Although at the early stages of a mission the uncertainty of prior knowledge might be large, this uncertainty is reduced over time using the Bayesian updating framework. Additionally, the changes to a mission plan, such as an increase in the duration of the mission, can be incorporated into the adaptive prediction. Some preliminary simulation results based on this proposed approach have been already presented Sadrpour et al. (2012).

3. METHODOLOGY

3.1. Overview of Methodology

Figure 1 shows the framework of the proposed two approaches. A Bayesian regression model is used for predicting the mission power when prior knowledge of the road segments is available. In this paper, a road segment is defined as a part of a road that has a consistent average grade and a consistent surface condition. For comparison, a linear regression is used when there is no prior knowledge of the mission. In both approaches, the model parameters are recursively updated based on real-time measurements of the instantaneous UGV velocity and energy consumption. The updated model is used to predict the future power consumption. Finally, the probability of successfully accomplishing the mission can also be adaptively estimated during the mission execution.

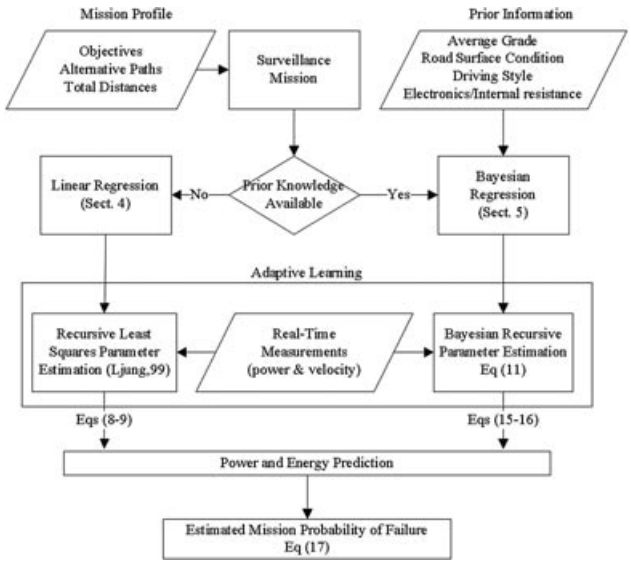

Figure 1. Overview of methodology for prediction of mission energy.

3.2. Vehicle Dynamic Model

A vehicle longitudinal dynamics model, as typically used for power consumption studies in automobiles, is also utilized here (Ulsoy et al. 2012). The UGV power consumption is mainly associated with five key factors: (i) road grade (road profile), (ii) road surface condition (rolling resistance), (iii) driving style (velocity and acceleration profiles), (iv) vehicle internal resistances, and (v) sensors and electronic equipment as follows:

$$P(t) = F(t)u(t) + b = \underbrace{(W\sin(\theta(t))}_{\text{(i)}} + \underbrace{f\,W\cos(\theta(t))}_{\text{(ii)}} + \underbrace{ma(t)}_{\text{(iii)}} + \underbrace{C_I}_{\text{(iv)}})u(t) + \underbrace{b}_{\text{(v)}} + \varepsilon(t), \quad (1)$$

where $P(t)$ is the power at time t, $F(t)$ is the total traction force, $u(t)$ is the velocity, m is the vehicle mass, $a(t)$ is the acceleration, W is the vehicle weight, $\theta(t)$ is the road grade, f is the road rolling resistance coefficient, C_I is the internal resistance coefficient, b represents other constant sources of energy depletion, such as electronic sensors onboard the vehicle, and $\varepsilon(t)$ is the model error. Other time-varying factors, which have a smaller relative significance, such as aerodynamic drag, are neglected here due to the low operating speed of small UGVs.

Equation (1) is nonlinear with respect to the parameter θ. Since in most applications the road grade does not exceed 15 degrees, it can be linearized as follows:

$$P(t) = F(t)u(t) + b = (W\theta(t) + fW + ma(t) + C_I)\,u(t) + b + \varepsilon(t). \quad (2)$$

This linearization or the point about which we linearize the model does not introduce limitations in the methodology or the prediction approaches (see Sections 4.1 and 5.1). Equation (2) can be rewritten as a linear regression model:

$$P(t) - ma(t)u(t) = u(t)W(\theta(t) + f + C_I^{'}) + b + \varepsilon(t), \quad (3)$$

where the left side of Eq. (3) can be generally denoted as the response $y(t)$, i.e., $y(t) = P(t) - ma(t)u(t)$; $u(t)W$ is considered as the predictor denoted by $x(t)$; and $C = \theta(t) + f + C_I^{'}$ is the regression model parameter that combines the grade, rolling resistance coefficient, and internal frictional losses. For ease of notation and without loss of generality, we have defined $C_I^{'} = C_I/W$. Although $C_I^{'}$ is not as physically meaningful as C_I, this factorization allows us to preserve the physical meaning of θ and f, which are the major components of the prior knowledge. Thus,

$$y(t) = b + Cx(t) + \varepsilon(t). \quad (4)$$

In practice, the actual instantaneous UGV power consumption can be obtained in real-time by multiplying the measured current and voltage of the battery. The vehicle velocity can also be measured using a wheel velocity encoder. The acceleration can be estimated based on the difference between two consecutive velocity measurements. Generally, the exact values of rolling resistance coefficient, road grade, and vehicle internal resistance are difficult to know beforehand; however, some rough knowledge of the vehicle characteristics and road conditions, which can be generally expressed by a prior probability distribution, might be available. The modeling error term, $\varepsilon(t)$, is assumed to follow an $i.i.d.$ normal distribution with zero mean and variance that is estimated by offline calibration experiments.

The proposed vehicle model has a few key properties. Equation (1) is a model based on vehicle-fixed coordinates, which implies movement along the heading direction of the vehicle (Ulsoy et al. 2012). Even when the vehicle heading changes, it still moves along a particular trajectory from which real-time measurements are collected, allowing the predictions to account for maneuvers such as turning. If a novice operator makes frequent turns, the estimated parameters of the model will increase and adapt to reflect the driving style of the operator. A limitation of the vehicle model is that the combined parameter, i.e., C, can algebraically become negative when a road grade is highly negative, and the road coefficient of rolling resistance is small (e.g., paved roads). In such extreme scenarios, the energy requirement for locomotion is very small, and if regenerative breaking capabilities are included in the vehicle design, a paved steep downhill road can be used for recharging the UGV batteries. However, power regeneration is rarely used in existing UGVs. Consequently, here, C is assumed to be non-negative. A road segment with a zero C indicates a negligible power requirement for locomotion as gravitational pull is large enough to overcome the rolling resistance of the road, resulting in a very small energy requirement for propulsion.

Figure 2. UGV on a mission with no prior knowledge.

4. APPROACH 1: LINEAR REGRESSION IN THE ABSENCE OF PRIOR KNOWLEDGE

4.1. Linear Regression for Power Prediction

In the absence of prior knowledge, the power consumption is predicted using the regression model (4). Figure 2 shows a simple representation of a hypothetical mission. The measurements are collected at discrete time intervals that are indexed by $k = 1, 2, ..., n$. The sampling interval is Δt, and the remaining distance of the mission is denoted by R; $t_e = n\Delta t$ is the end time of the mission. The combined parameter, C, and b are both updated based on real-time power and velocity measurements using RLS estimation with forgetting factor λ_{ff} (Ljung, 1999). By tuning the forgetting factor, we increase or decrease the impact of past measurements on the estimated parameters of the model. This allows RLS to adapt more quickly to changes in the operating conditions. Unlike Bayesian estimation, RLS does not require the linearization introduced by Eq. (2). The parameters of the model are not estimated individually; instead, a combined parameter $C_n = \sin(\theta(t)) + f\cos(\theta(t)) + C_I'$ is recursively estimated, where C_n is the nonlinear version of C. Also, RLS does not assume constant linear parameters during the mission execution. The parameters of the model are estimated adaptively, which can be considered as a piecewise linear estimation approach.

4.2. EWMA Control Chart Monitoring

The regression model parameters can adapt to small shifts and drifts in the power consumption when RLS estimation is used, but the adaptation can be slow when an abrupt change occurs such as at the onset of transition from one road segment to another. To overcome this shortcoming, an exponentially weighted moving average (EWMA) control chart is used to monitor the prediction residuals according to Montgomery (2005). The EWMA monitoring statistic,

$z(k)$, is defined as follows:

$$z(k) = \lambda_c \hat{e}(k) + (1 - \lambda_c) z(k-1),$$
$$\hat{e}(k) = y(k) - \hat{y}(k), \tag{5}$$

where λ_c is the EWMA weight and $\hat{y}(k)$ is the prediction of the response at k, e.g., $\hat{y}(k) = E[y(k)|x(k), \hat{C}(k-1), \hat{b}(k-1)]$, where $\hat{C}(k-1)$ and $\hat{b}(k-1)$ are the estimated parameters at $k-1$. When an out-of-control signal is detected, the RLS covariance matrix is reset to its initial (large) value.

4.3. Prediction of Mission Energy Requirement

To predict the total mission energy, the future values of the velocity are required, which can be estimated based on the driving style of the UGV operator. The velocity is forecast using exponential smoothing (EWMA) with a weight λ_u as discussed in Appendix A.1. Although the variance of velocity prediction error is considered in computing the energy prediction variance, we assume that the combined parameter, i.e., $\hat{C}(k)$, and $\hat{b}(k)$ are both deterministic with values equal to the most recent estimates of C and b for energy prediction. We make this assumption considering the smaller variance of estimated parameters compared to the variance of the predicted velocity.

The effect of driving style, i.e., the $ma(t)u(t)$ term in Eq. (1), is considered in the estimation of the combined parameter. However, its contribution to the overall energy consumption, which is denoted as $\eta = \frac{\int ma(t)u(t)dt}{\int p(t)dt}$, is very small (i.e., less than 1%), as shown in Figure 3. Thus, we can assume that the approximation of $\hat{y}(k+j|k) \approx \hat{P}(k+j|k)$ is reasonable for power prediction, where $\hat{y}(k+j|k)$ and $\hat{P}(k+j|k)$ are the j-step-ahead prediction of response and power at k. More specifically, $\hat{y}(k+j|k) = E[y(k+j)|x(1:k), \hat{C}(k), \hat{b}(k)]$, where $x(1:k)$ is the vector of available measurements from 1 to k.

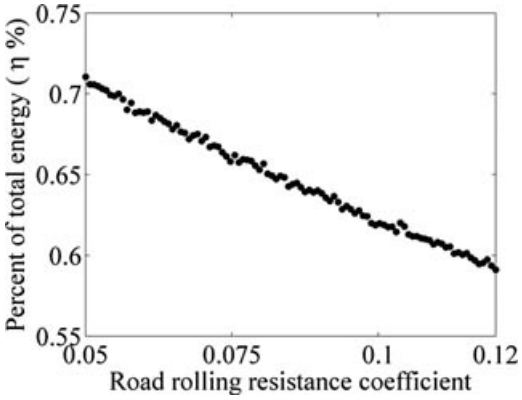

Figure 3. Percent of total energy associated with the driving style [i.e., $ma(t)u(t)$] term in Eq. (1) on a road segment with various levels of roughness and five degrees uphill grade with scaled EPA US06 speed profile shown in Figure 4. The power data were generated using Eq. (1) and the total energy was obtained using Eq. (6) assuming a 1-s sampling time.

Generally, we have some prior knowledge about the distance that the UGV will traverse. Additionally, the position of the UGV can be tracked via GPS, and the distance that the UGV needs to travel can be calculated. Therefore, the duration of a mission, i.e., t_e, can be estimated, denoted by $\hat{t}_e$, based on the remaining distance and real-time velocity measurements. The energy consumption can be calculated by integrating the instantaneous power over the duration of the mission as follows:

$$E_m = \int_0^{t_e} P(t)dt \approx \sum_{j=1}^{n} P(j)\Delta t. \tag{6}$$

Here, Δt is the sampling time, $t_e = n\Delta t$, and E_m is the total energy requirement for the mission, which can be estimated by

$$\hat{E}_m(k) = E_c(k) + \hat{E}_{rm}(k), \tag{7}$$

where $E_c(k)$ is the energy consumed up to time $t = k\Delta t$, and $\hat{E}_{rm}(k)$ is the expected energy requirement for the remainder of the mission. Using Eqs. (6) and (7), the expected total mission energy and the corresponding variance at k can be estimated as detailed in Appendix A.2:

$$\hat{E}_m(k) = \left(\sum_{j=1}^{k} P(j) + \sum_{j=1}^{\hat{n}-k} \hat{P}(k+j|k) \right) \Delta t$$
$$= E_c(k) + (\hat{n} - k) \left(W\hat{u}(k+1|k)\hat{C}(k) + \hat{b}(k) \right) \Delta t, \tag{8}$$

$$\mathrm{var}(\hat{E}_m(k)) = \left(\sum_{j=1}^{\hat{n}-k} var(P(k+j|k)) \right) (\Delta t)^2. \tag{9}$$

Equation (9) can be used to calculate the 95% prediction upper and lower confidence intervals, i.e., *UCI* and *LCI*.

5. APPROACH 2: BAYESIAN ESTIMATION AND PREDICTION IN THE PRESENCE OF PRIOR KNOWLEDGE

5.1. Bayesian Estimation

Mission prior knowledge consists of (a) road grade information, (b) road rolling resistance information, (c) constant power consumption information due to sensors and electronic equipment, (d) vehicle internal resistance, and (e) driving style. The prior knowledge of electronic component power consumption and the vehicle internal resistance is obtained from the manufacturer or by using offline calibration experiments (Sadrpour et al., 2013). The mission prior knowledge is also affected by the operating condition of the mission. For instance, a mission conducted at night will

Table I. Experimentally established prior knowledge (Sadrpour et al., 2013).

Prior distribution of average road grade (degrees)			Prior distribution of rolling resistance coefficient		
Road grade	Mean	Standard deviation	Road conditions	Mean	Standard deviation
Steep-Uphill	8	3	Sidewalk	0.056	0.025
Uphill	4	2	Asphalt	0.062	0.026
Flat	0	2	Tile	0.066	0.025
Downhill	−4	2	Grass	0.099	0.025
Steep-Downhill	−8	3			
Vehicle Parameters					
	Mean	Standard deviation		Mean	Standard deviation
Internal resistance	0.22	0.003	Sensors & Electronics	28.29	1.73

require infrared cameras, while in daylight there is no such need. Such information can be incorporated in the estimation of b in Eq. (4) using the Bayesian framework. A normal distribution is used to represent the prior information of b. The variance of the prior distribution represents the uncertainty of prior knowledge. The other two categories of prior information, i.e., road grade and rolling resistance, are divided into subcategories as shown in Table I.

The values for rolling resistance coefficients in Table I were obtained by offline experiments using the PackBot and collecting data from several road segments of different road types. For more details of the experiments, see Sadrpour et al. (2013). The design of the prior knowledge table for the road grade was motivated by visual perception. It has been shown that human visual perception of a road grade is biased toward overestimation (Proffitt et al. 1995). In our experiments, we could comfortably visually discern the flat roads, average slopes of up to $\pm 3^\circ$, from roads with slopes of $\pm 3^\circ$, $\pm 5^\circ$ degrees, labeling them as up/downhill. Similarly, roads with slopes ranging from $\pm 6^\circ$ to $\pm 12^\circ$ visually appeared to be steep up/downhill, although our verbal estimates of the grade were higher than the measured grade. Thus, while the visual perception of the numerical value of the slope may be biased, it was able to effectively classify roads into the correct categories of flat, up/downhill, and steep up/downhill. For instance, an operator may state that the next road segment of the mission is on average flat and the road surface is grass. This prior information is matched with its associated prior distributions in Table I. The normal distribution is used to represent the prior information for each parameter subcategory. The variances of the prior distributions are estimated by experiment, but rough estimates can also be extracted from the literature (Wong, 2008). Also, the prior information of the average vehicle velocity during the mission is obtained by requesting the operator to indicate his or her driving style, as shown in Table II. For instance, a moderate driver is expected to operate the UGV at an average velocity of 1–2 m/s.

Table II. Driving style prior information (average speed).

Driving type	Conservative	Moderate	Aggressive
u	0-1 m/s	1-2 m/s	2-3 m/s

Based on Eq. (3), the prior distribution of C can be expressed as follows:

$$C_i^0 = f_i^0 + \theta_i^0 + C_I'^0 \sim N\Big(\mu_{f_i}^0 + \mu_{\theta_i}^0 + \mu_{C_I'}^0, \left(\sigma_{f_i}^0\right)^2 + \left(\sigma_{\theta_i}^0\right)^2 + \left(\sigma_{C_I'}^0\right)^2\Big), \tag{10}$$

where $\mu_{f_i}^0$, $\mu_{\theta_i}^0$, and $\mu_{C_I'}^0$ are the means of the prior distributions of rolling resistance coefficient, average grade, and vehicle internal resistance, respectively, for road segment i, and $(\sigma_{f_i}^0)^2$, $(\sigma_{\theta_i}^0)^2$, and $(\sigma_{C_I}^0)^2$ are the corresponding variances of the prior distributions. Unlike RLS, here the linearization affects the distribution of the combined parameter. The linearization around $\theta = 0$ resulted in $C = \theta + f + C_I'$; however, we could linearize Eq. (1) about the operating condition of the prior mean. This would have resulted in a different relationship between C, f, θ, C_I', and also a different model for each operating condition. The resulting model would have still been linear, so the proposed Bayesian prediction could be applied. Experimental validation (Sadrpour et al., 2013) showed that the linearization about $\theta = 0$ is adequate for prediction of power under typical operating conditions, i.e., $|\theta| \leq 12^\circ$. Also, operating in roads with more extreme uphill or downhill grades resulted in robot slippage and tipping. We assume that the prior distributions of C_i and b_i are independent, and $\sum_{C_i,b_i}^0 = \begin{bmatrix} (\sigma_{b_i}^0)^2 & 0 \\ 0 & (\sigma_{C_i}^0)^2 \end{bmatrix}$ represents their prior covariance matrix.

Assume that a mission is composed of $i = 1, 2, \ldots, s$ road segments as shown in Figure 5; R_i represents the remaining distance of road segment i; n_i and $t_i = n_i \Delta t$ are the

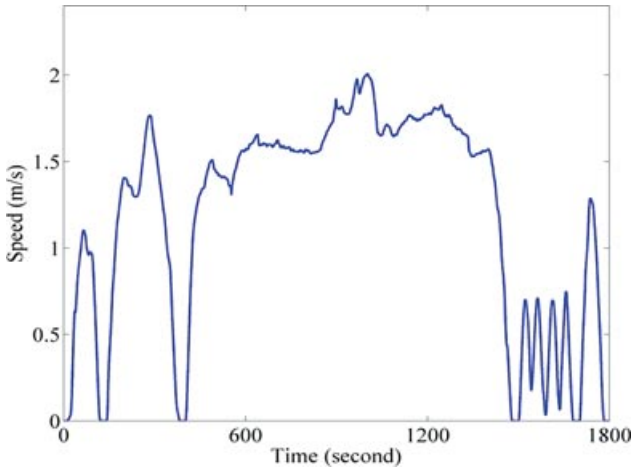

Figure 4. Drive cycle based on a scaled EPA US06 is used for simulation studies.

final measurement index and the end time of road segment i, respectively.

The posterior distribution of C_i and b_i at k ($n_{i-1} < k \leq n_i$) can be obtained recursively based on the measurements only from its road segment (Congdon, 2003):

$$\begin{aligned}\hat{\Sigma}_{\boldsymbol{\beta}_i}(k|n_{i-1}+1:k) &= (\boldsymbol{x}^T(k)\boldsymbol{x}(k)\sigma_\varepsilon^{-2} \\ &\quad + \hat{\Sigma}_{\boldsymbol{\beta}_i}^{-1}(k-1|n_{i-1}+1:k-1))^{-1}, \\ \hat{\mu}_{\boldsymbol{\beta}_i}(k|n_{i-1}+1:k) &= \hat{\Sigma}_{\boldsymbol{\beta}_i}(k|n_{i-1}+1:k)(\boldsymbol{x}^T(k)y(k)\sigma_\varepsilon^{-2} \\ &\quad + \hat{\Sigma}_{\boldsymbol{\beta}_i}^{-1}(k-1|n_{i-1}+1:k-1) \\ &\quad \times \hat{\mu}_{\boldsymbol{\beta}_i}(k-1|n_{i-1}+1:k-1)), \quad (11)\end{aligned}$$

where for ease of notation we have defined $x(k) = [1\ x(k)]$ and $\hat{\mu}_{\beta_i}(k|n_{i-1}+1:k) = [\hat{\mu}_{b_i}(k|n_{i-1}+1:k)\ \hat{\mu}_{C_i}(k|n_{i-1}+1:k)]$, and $\hat{\mu}_{\beta_i}(k|n_{i-1}+1:k)$ and $\hat{\Sigma}_{\beta_i}(k|n_{i-1}+1:k)$ represent the $(k-n_{i-1})^{th}$ update of the mean and covariance matrix of b_i and C_i, respectively. The initial values of the mean and variance are obtained according to Eq. (10). On road segment i, n_{i-1} has been observed and is not estimated.

Before any measurements are collected from a road segment, the power prediction distribution for road segment i has a normal distribution as follows (see Appendix A.3):

$$P_i(j|0) \sim N(Wu^0\mu_{C_i}^0 + \mu_{b_i}^0, (W\mu_{C_i}^0)^2\mathrm{var}(u(j|0)) + \sigma_\varepsilon^2). \quad (12)$$

Equation (12) is conditioned on the mission prior knowledge of $\mu_{b_i}^0, \mu_{C_i}^0$, u^0, and $\mathrm{var}(u(j|0))$ where $\mu_{C_i}^0$ is the prior mean of the combined parameter according to Eq. (10) u^0 is the velocity prior value obtained from Table II, and $\mathrm{var}(u(j|0))$ can be obtained as described in Appendix A.1.

When measurements are collected from a road segment, the power prediction distribution is sequentially updated. The combined parameter and constant energy terms are assumed to be deterministic and equal to the posterior mean, e.g., $\hat{\mu}_{b_i}$ and $\hat{\mu}_{C_i}$. For instance, the power prediction distribution for road segment i at k ($n_{i-1} < k \leq n_i$) can be shown to be normally distributed (see Appendix A.3) as follows:

$$P_i(k+j|k) \sim N(\hat{\mu}_{p_i}(k+j|k), \hat{\sigma}_{p_i}^2(k+j|k)), \quad (13)$$

where

$$\begin{aligned}\hat{\mu}_{p_i}(k+j|k) &= W\hat{u}(k+j|k)\hat{\mu}_{C_i}(k|n_{i-1}+1:k) \\ &\quad + \hat{\mu}_{b_i}(k|n_{i-1}+1:k), \\ \hat{\sigma}_{p_i}^2(k+j|k) &= (W^2\hat{\mu}_{C_i}^2(k|n_{i-1}+1:k)\,\mathrm{var}\,(u(k+j|k)) + \sigma_\varepsilon^2.\end{aligned}$$

5.2. Prior Updating for Future Missions Based on Past Measurements

An additional advantage of the Bayesian prediction framework is that the information uncertainty about the mission operating condition can be improved over time as the UGV traverses more road segments. The prior distributions of the combined parameters, presented in Table I, can be updated based on the measurements from earlier road segments. Initially, the prior values of the rolling resistance coefficients, the vehicle internal resistance, and sensors and electronic equipment in Table I might not be accurate for the specific UGV or mission. However, these values are continuously updated during the execution of the mission. The combined parameter's posterior distribution can be used as the prior

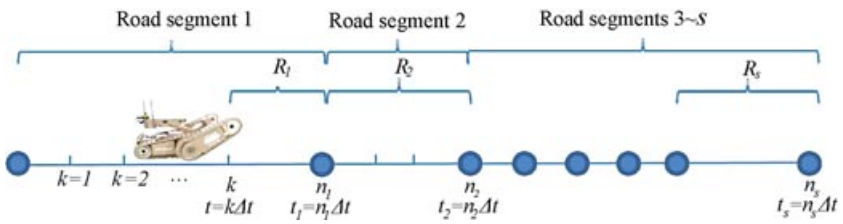

Figure 5. UGV on a mission comprised of s road segments.

distribution for the road segments in future missions when a similar combination of road grade and surface condition is encountered.

In addition to updating the combined parameter distribution, the prior distributions of rolling resistance coefficients can be updated. A very likely scenario is when the UGV returns to its initial location at the end of a mission through the same road segment it initially undertook. An uphill road segment in the departure trip usually means a downhill road segment in the return trip. If the combined parameter of the road segment in the departure trip is represented as $C_i = f_i + \theta_i + C_I^{'}$, then $C_j = f_i - \theta_i + C_I^{'}$ represents the combined parameter in the return trip from the same road segment. Thus, $\left(C_i + C_j\right) / 2$ provides an estimate of the road rolling resistance and vehicle internal resistance coefficient $f_i + C_I^{'}$. Since the internal resistance, i.e., $C_I^{'}$, is independent of the road segment surface condition and grade, it is convenient to think of $f_i + C_I^{'}$ as one parameter and carry out predictions. This approach allows us to update the prior distribution of $f_i^0 + C_I^{'0}$ for future missions.

5.3. Prediction of Mission Energy Requirement

The mission total energy requirement has three parts:

$$\hat{E}_m(k) = E_c(k) + \hat{E}_{rs_i}(k) + \sum_{\ell=i+1}^{s} \hat{E}_{s_\ell}(k), \tag{14}$$

where $\hat{E}_{rs_i}(k)$ is the prediction of the energy requirement for the remainder of the i^{th} road segment and $\hat{E}_{s_\ell}(k)$ is the prediction of the energy requirement for the future road segment ℓ ($\ell > i$). At k,($n_{i-1} < k \leq n_i$), the expected values of $\hat{E}_{rs_i}(k)$ and $\hat{E}_{s_\ell}(k)$ are

$$\hat{E}_{rs_i}(k) = (\hat{n}_i - k)(W\hat{u}(k+1|k)\hat{\mu}_{C_i}(k|n_{i-1}+1:k) + \hat{\mu}_{b_i}(k|n_{i-1}+1:k))\Delta t, \tag{15}$$

$$\hat{E}_{s_\ell}(k) = (\hat{n}_\ell - \hat{n}_{\ell-1})(W\hat{u}(k+1|k)\mu_{C_\ell}^0 + \mu_{b_\ell}^0)\Delta t. \tag{16}$$

The variance of prediction is computed according to Appendix A.3. The predicted energy is updated sequentially with real-time measurements, and the probability of completing the mission given the stored energy in the UGV batteries is calculated. If the estimated total energy requirement exceeds the failure threshold, i.e., E_{th}, it indicates that the UGV will exhaust its energy before completing its mission. The mission completion probability, at time step k, can be estimated by

$$\Pr(\hat{E}_m(k) \leq E_{th}). \tag{17}$$

5.4. Application Scope of Proposed Methods

The prediction methodologies previously introduced can be applied to a variety of scenarios, and the scope and range of their applications are discussed next. The naive approach, which was introduced in the introduction, does not require a model for making predictions; however, unlike our proposed methods, it does not consider any information about the road surface condition changes. Therefore, the naive approach can neither handle situations when the characteristics of a road surface suddenly change, nor provide an estimate of the energy prediction uncertainty.

Compared to the naive approach, the RLS approach is based on a stochastic model and adapts more quickly to both large and small changes in operating conditions using a forgetting factor and covariance resetting. Also, since it uses the vehicle model for prediction, it provides an estimate of prediction uncertainty. However, both the RLS and naive approaches only use real-time measurements for prediction without considering the available prior knowledge of road conditions.

In the absence of prior knowledge, the Bayesian approach will resemble the RLS approach. However, when prior knowledge is available, the Bayesian approach typically outperforms RLS even with moderately imprecise prior knowledge. Moreover, the Bayesian approach is most valuable when the following conditions are satisfied: (a) the energy requirement for locomotion accounts for a large percentage of the total energy requirement for completion of the mission. If this condition is not true, the impact of variations in road condition and its prior information on the overall energy will be small. If electronic components onboard the vehicle consume the majority of energy instead, other strategies can be utilized to minimize the energy consumption (Mei et al. 2005). (b) The internal resistance of the vehicle is not so large as to overshadow the energy requirement for overcoming the road rolling resistance and grade (see Section 6.2). (c) Road segments are structured, such as paved and unpaved surfaces made of grass, asphalt, and cement, and indoor surfaces, e.g., carpet and tile. However, road surfaces that are unstructured, such as earthquake-affected areas, a forest floor with many obstacles, or roads whose surface condition or grade change very often, are difficult to characterize or to obtain reliable prior information about.

6. EXPERIMENTAL AND SIMULATION STUDIES

In Sadrpour et al. (2013), we conducted experimental tests using the PackBot to validate several key aspects of the proposed prediction approaches: (a) the linear approximation of the vehicle longitudinal dynamic model with respect to velocity and grade was validated, (b) statistical tests were used to categorize and classify typical surface types based on their rolling resistances, (c) procedures for collecting prior knowledge in the Bayesian approach were

Table III. Features presented in the study.

Study	Type	Mission type	Feature presented in the simulation
1	Experiment	Short	Precise mission prior knowledge
2	Experiment	Short	Imprecise mission prior knowledge
3	Simulation	Long	In-advance parameter updating

discussed and validated, (d) the RLS and Bayesian prediction approaches were validated and compared, showing that the Bayesian estimation outperformed RLS as expected.

In this section, a few surveillance scenarios are used to illustrate different features of the proposed methods shown in Table III. First, we demonstrate and compare the performances of the RLS and Bayesian prediction approaches when precise prior knowledge of the mission is available. We demonstrate that improved predictions are achievable in the Bayesian approach even with moderately imprecise mission prior knowledge. Additionally, since the vehicle dynamic model was validated in Sadrpour et al. (2013), we use the model to generate surrogate scenarios in which the imprecise prior knowledge can be corrected *in-advance* by using the similarities among road segments in a round-trip mission. In each study, the mission energy requirement is predicted and updated using Eqs. (8) and (9) when prior knowledge is unavailable and Eqs. (15) and (16) when prior knowledge is available. In addition, the 95% confidence intervals in each case are computed according to Appendix A.4. The two surveillance scenarios that are used for these studies are as follows:

1. *Short (surveillance) mission:* This scenario was carried out using a small-size UGV. The mission is composed of two road segments as shown in Figure 6. In this mission, the UGV visits A-B-C, respectively. The robot uses two different road segments to accomplish this mission. The first road segment is a downhill sidewalk, and the second road segment is a flat grass field.
2. *Long (surveillance) mission:* The vehicle dynamic model is used to generate power data for this scenario. The mission is composed of four road segments as shown in Figure 7. During the round-trip mission, the UGV visits points A-B-C-B-A, respectively. The path from A to B is steep uphill and from B to C is downhill. Unlike the short mission scenario, in this round trip, the vehicle returns to its initial location using the same road segments, e.g., A-B-C and C-B-A are the same. Thus, the rolling resistance and road surface condition are assumed to be consistent for all the road segments in the long mission. The prior parameters of each road segment are also depicted.

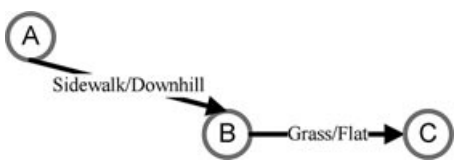

Figure 6. The short mission is composed of two road segments.

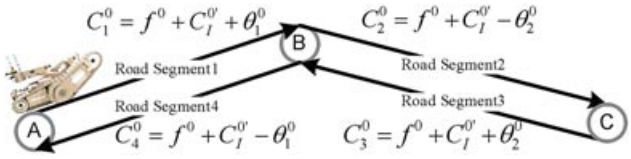

Figure 7. The long mission (a round trip) is composed of four road segments.

6.1. Experimental Study 1: Impact of Mission Prior Knowledge on Energy Prediction

The goal of this experimental study is to demonstrate the advantage of using mission prior knowledge in predicting the mission energy requirement. The robot used for this study is the PackBot (Figure 8) manufactured by iRobot. The robot is maintained by the Ground Robotics Reliability Center at the University of Michigan in Ann Arbor. The communication between the operator and the UGV is through a C programmable application programming interface, which is used to control the robot and acquire the measurement data in real-time.

In this scenario, the drive cycle shown in Figure 4, the scaled aggressive EPA US06, was prescribed to the PackBot. The first road segment was a downhill sidewalk (−3 degrees on average) and the second road segment was a flat grass field. For details of the test plan and data collection procedures, see Sadrpour et al. (2013). The corresponding power consumption profile, which is shown in Figure 9, was measured for both road segments. Next, the prediction approaches were applied to the data using the prior knowledge information presented in Table IV. The mission schematic is shown in Figure 6.

In Figure 10, the estimated *total* mission energy, $\hat{E}_m(k)$, and the corresponding 95% upper and lower confidence intervals, i.e., *UCI* and *LCI*, based on the RLS approach are compared against that of the Bayesian approach. In addition, we have shown the prediction based on the naive approach introduced in the introduction. The naive approach only provides an estimate of the expected energy requirement using the relationship $\hat{E}_m(k) = E_c(k) + \overline{P}(k)(\hat{t}_e - k\Delta t)$, where $\overline{P}(k)$ and $(\hat{t}_e - k\Delta t)$ are the average power measurements up to time k using the current draw and voltage of the battery, and the estimated remaining duration of the mission, respectively. Letters A, B, and C indicate the position of the UGV in the mission as shown in Figure 6. An out-of-control signal (covariance resetting) occurs at the onset of the transition from the sidewalk road to the grass field about

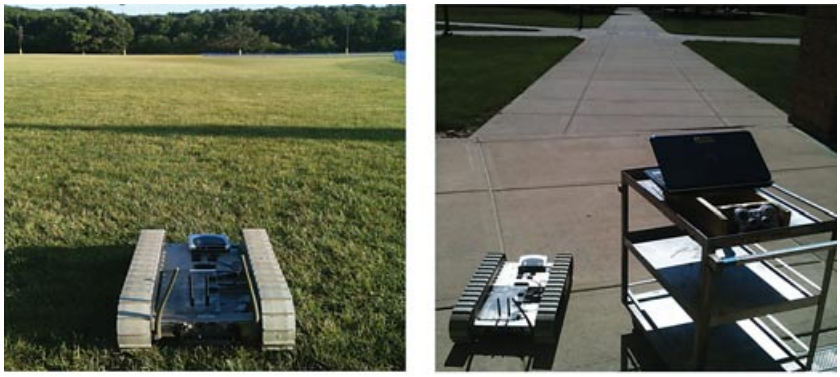

(a) (b)

Figure 8. The PackBot used on a grass surface and a sidewalk surface for power data collection.

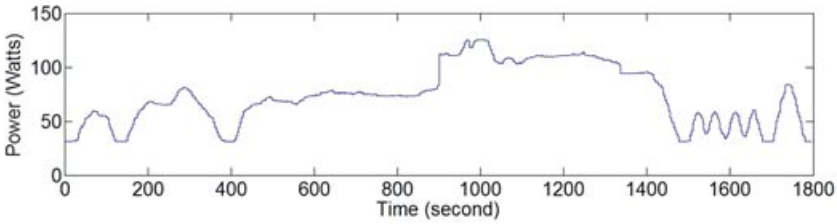

Figure 9. UGV power profile

15 min into the mission. The naive approach has the least accurate prediction throughout the mission, but the RLS approach also excessively underestimates the mission energy requirement in the first road segment due to lower power consumption in the first road segment compared with the second road segment. This problem is resolved when the measurements from the second road segment are collected and predictions quickly converge to the actual total mission energy requirement, i.e., $\hat{E}_a$. The Bayesian predictions take advantage of the prior knowledge of the second road segment before its actual measurements become available, which results in more accurate predictions, allowing the operator to prevent unanticipated mission failures due to a shortage of energy.

The failure threshold, E_{th}, can be defined to be 1.5 times the expected total mission energy based on the initial prior information. Relying on the real-time data alone in the RLS approach may result in misdetection of failures at the initial stage of the mission since the predicted end-of-mission energy is far below the failure threshold. In contrast, the Bayesian approach provides more accurate predictions, allowing the operator to prevent unanticipated mission failure due to a shortage of energy.

Table IV. Parameters of Experimental Study 1.

Parameters	Value
Sidewalk surface prior parameters $(\mu_{f1}, \sigma_{f1}^2)$	$(0.056, 0.025^2)$
Grass surface prior parameters $(\mu_{f2}, \sigma_{f2}^2)$	$(0.099, 0.025^2)$
Sidewalk grade prior (downhill) $(\mu_\theta, \sigma_\theta^2)$	$(-4, 2^2)$ degrees
Grass grade prior (flat) $(\mu_\theta, \sigma_\theta^2)$	$(0, 2^2)$ degrees
UGV mass	35 lb
Road segments length	1074 m
λ_{ff}	0.98
λ_u	0.002
σ_ϵ	5 W
Sampling time Δt	3 s

6.2. Experimental Study 2: Effect of Mission Imprecise Prior Knowledge on Energy Prediction

The impact of imprecise prior knowledge on the mission energy prediction is studied here. The scenario of the first study is used again. The vehicle parameters in Table I are estimated by offline experiments and do not vary from one mission to another. However, other parameters in the table are obtained from the operator and change depending on the mission characteristic. Thus, they are more likely to be subject to operator misperception. In this study, we consider the type of imprecision that arises from inaccurate prior information regarding the road surface type or the road grade.

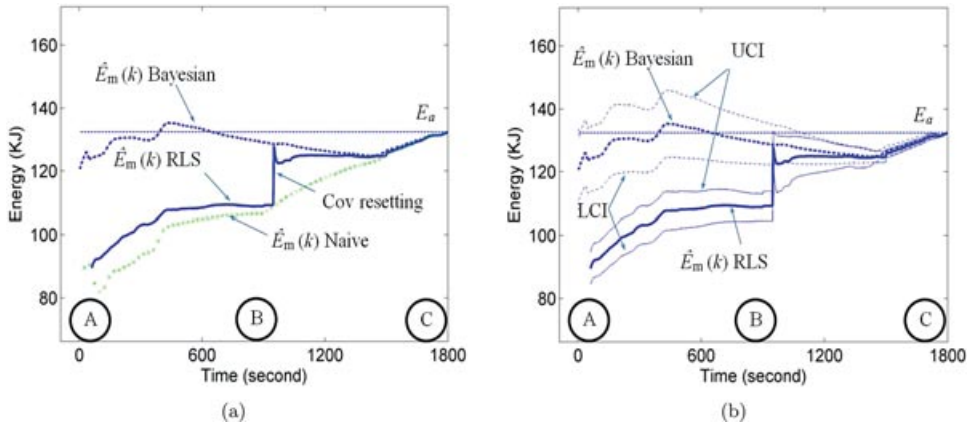

Figure 10. (a) Energy prediction mean vs. time using the Bayesian, RLS, and naive approaches. Unlike Bayesian predictions, the naive and RLS approaches underestimate the mission energy requirement. The dashed line at 135 KJ indicates the actual total energy consumed for the mission, E_a. (b) Energy prediction vs. time using the Bayesian and RLS approaches with prediction confidence intervals utilizing correct prior information.

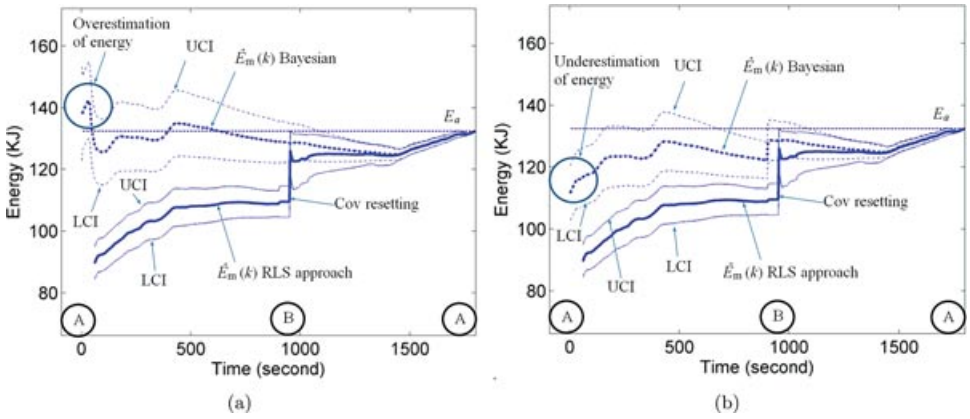

Figure 11. (a) Categorizing the first road segment as flat-grass instead of downhill-sidewalk results in an overestimation of power consumption in the Bayesian approach, which is quickly corrected with a few measurements from the road. The Bayesian approach still outperforms the RLS approach. (b) Categorizing the second road segment as sidewalk instead of grass results in an underestimation of power consumption in the Bayesian approach. The Bayesian predictions still outperform the RLS predictions, but the underestimation cannot be corrected while traversing the first road segment.

In the Bayesian approach, imprecise prior knowledge can lead to less accurate predictions. For instance, categorizing the downhill-sidewalk road as flat-grass for the first road segment will result in an overestimation of the mission energy requirement, as shown in Figure 11(a). Since actual measurements can be collected from this road segment quickly after the start of the mission, the poor prior information is corrected after a few measurements. However, if the prior knowledge of the second road segment is imprecise, for instance categorizing the grass road as sidewalk, the predictions cannot be corrected until measurements are collected from that road segment at the end of the first road segment, as shown in Figure 11(b). Even in this case, the Bayesian prediction still typically outperforms the RLS. In the first road segment, the RLS approach, which does not use the mission prior knowledge, assumes that the remaining mission, including the second road segment, is a downhill sidewalk similar to the past observations.

In the Bayesian approach, miscategorizing the second road segment as sidewalk still leads to an estimate of the combined parameter that is closer to its actual value compared to the linear regression approach because of the correct prior knowledge about the road grade. As long as the prior knowledge yields parameter estimates that are closer to the true parameters compared to the case of not having any prior knowledge, i.e., the RLS approach, the Bayesian predictions will outperform the RLS predictions.

The criticality of the prior information of the road grade and the rolling resistance after the start of a mission and data collection can be intuitively assessed using the linearized vehicle dynamic model (3) and (4). Both the RLS and the Bayesian approaches can estimate parameter b in the model accurately using the real-time data. Thus, the advantage of the Bayesian approach lies in the combined parameter C. Two factors can weaken the importance of mission prior knowledge (a) The weight of the vehicle: If the vehicle is very light, the ratio of $\frac{Cx(t)}{b}$ becomes small, and so does the importance of C in the overall energy consumption of the vehicle (b) The internal resistance of the vehicle: If the internal resistance, $C_I^{'}$, is too large, it will dominate the effect of $\theta + f$, reducing their importance in the overall energy consumption. In these two cases, the difference between the RLS and the Bayesian predictions will be less pronounced.

6.3. Simulation Study: In-advance Parameter Updating Using the Vehicle Surrogate Model

In some commonly encountered scenarios, such as the long mission scenario shown in Figure 7, it is possible to update the imprecise prior knowledge of road segments in the Bayesian approach *in-advance* before actual measurements are collected based on similarities among roads. The goal of this simulation study is to demonstrate this capability. In-advance updating is performed using the concepts introduced in Section 5.2, which are listed in Table V. For instance when the UGV is on the first road segments, two in-advance updating strategies are outlined in the first row of Table V.

Since the vehicle model was validated in Sadrpour et al. (2013), the power data are generated using the nonlinear vehicle dynamic model in Eq. (1) with the parameters shown in Table VI and the scaled EPA US06 drive cycle. The value of rolling resistance was generated from its corresponding prior distribution. Other parameters, such as road grade, vehicle internal resistance, and consumption of electronic components, are also assumed fixed, and the randomness in the simulated data is due to the $\varepsilon(t)$ term. The remaining parameters, i.e., the vehicle weight and the model noise variance, were previously presented in Table IV.

The accuracy of prior knowledge is critical for the in-advance updating introduced in the first two rows of Table V.

Table V. Strategies for in-advance updating of road combined parameter.

UGV position	Update 1	Update 2
Road segment 1(early)	$\hat{C}_4 = 2(f^0 + C_I^{'0}) - \hat{C}_1$	$\hat{C}_4 = \hat{C}_1 - 2\theta_1^0$
Road segment 2(early)	$\hat{C}_3 = 2(f^0 + C_I^{'0}) - \hat{C}_2$	$\hat{C}_3 = \hat{C}_2 - 2\theta_2^0$
Road segment 3	$\hat{C}_4 = \hat{C}_2 + \hat{C}_3 - \hat{C}_1$	$\hat{f} + \hat{C}_I^{'} = (\hat{C}_2 + \hat{C}_3)/2$

Table VI. Simulation parameters.

Simulation parameters	Value
Grass rolling resistance $\sim (0.099, 0.025^2)$	0.109
Segment 1 and 4 road grade ($\theta_{1,4}$)	±7.5 degrees
Segment 2 and 3 road grade ($\theta_{2,3}$)	±6 degrees
Internal resistance coefficient ($C_I^{'}$)	0.22
Sensors & Electronics (b)	28.29 W
Road segments length	537 m

This *early* in-advance updating should be carried out only if the prior knowledge of the road rolling resistance coefficients or average grade is accurate. As shown in Table V, $\hat{C}_3$ or $\hat{C}_4$ can be updated in two different ways. The first alternative, $\hat{C}_4 = 2(f^0 + C_I^{'0}) - \hat{C}_1$, should be used in scenarios with high confidence in the precision of f^0 and less confidence in θ_i^0, while $\hat{C}_4 = \hat{C}_1 - 2\theta_1^0$ should be used in scenarios with more confidence in the prior knowledge of θ_i^0 and less confidence in f^0. The in-advance updating introduced in the third row of Table V is entirely based on the estimated parameters and does not rely on the mission prior knowledge. Thus, $\hat{C}_4 = \hat{C}_2 + \hat{C}_3 - \hat{C}_1$ can be carried out even without precise prior knowledge of grade or rolling resistance.

Since early in-advance updating relies on precise prior knowledge, it is not utilized in this simulation, and we demonstrate the improvements by using only the update introduced in the third row of Table V. The prior information of this mission is shown in Table VII. We assume imprecise prior knowledge of f^0, i.e., categorizing the grass road as sidewalk. Additionally, although the grades of all four road segments are categorized correctly using the mission prior knowledge, the means of their corresponding prior distributions do not match with the grade parameter value that was used to simulate the data, shown in Table VI. Thus, the initial prior knowledge of combined parameters, i.e., C_i^0, $i = \{1, \ldots, 4\}$, is imprecise and does not match their true values.

Figure 12(a) compares the mission energy prediction for the long mission scenario using the Bayesian prediction approach with and without in-advance updating. Letters A through C indicate the position of the UGV corresponding to Figure 7. As shown in Figure 12(a), since early

Table VII. Prior information for simulation study.

Prior knowledge category	Operator response
First road segment average grade	Steep uphill
Second road segment average grade	Downhill
Third road segment average grade	Uphill
Fourth road segment average grade	Steep downhill
Road segments surface condition	Sidewalk (imprecise)
Driving style	Moderate

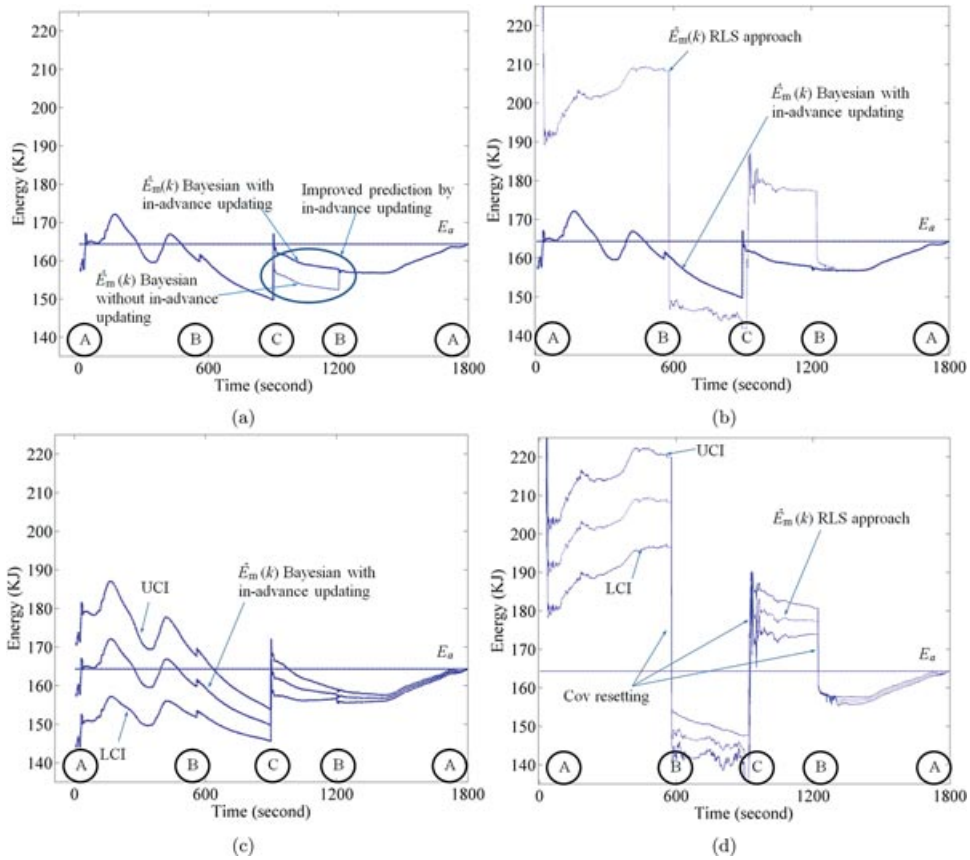

Figure 12. End-of-mission energy prediction vs. time. (a) Prediction mean vs. time with and without in-advance parameter updating using the Bayesian prediction approach. In-advance updating corrects the imprecise prior knowledge, resulting in more accurate predictions in the third road segment. (b) Prediction mean from the Bayesian approach with in-advance updating compared against the RLS prediction mean. The Bayesian prediction outperforms the RLS prediction in all road segments. (c) Bayesian prediction with in-advance updating with confidence intervals. (d) RLS prediction with confidence intervals.

in-advance updating is not used, the predictions in the first two road segments are identical in both approaches. Due to the imprecise prior knowledge of road condition, C_4^0 is underestimated and is corrected when the UGV is traversing the third road segment using the available measurements and in-advance updating $\hat{C}_4 = \hat{C}_2 + \hat{C}_3 - \hat{C}_1$. Figure 12(a) depicts more accurate results on the third road segment as a result of in-advance updating compared with the earlier approach without in-advance updating. The predictions on the third road segment converge to the proximity of the mission true energy requirement approximately 5 min earlier than the previous approach, which is a significant improvement for mission planning and an early detection of failure. Also, Figure 12(b) compares the mean of predictions in the Bayesian approach with in-advance updating against the RLS approach, and shows that the prediction based on the Bayesian approach is more accurate throughout the mission. Figures 12(c) and 12(d) depict the same predictions with the confidence intervals.

In practice, we expect round-trip missions, similar to the one presented in this study, to occur frequently, and We demonstrate the twofold benefit of the Bayesian approach in such scenarios: (a) direct use of prior knowledge to improve the prediction; (b) use of the mission overall structure to exploit the dependencies and similarities between road segments for in-advance updating of parameters.

7. SUMMARY AND FUTURE WORK

This paper has presented a general framework for predicting end-of-mission energy, which can help prevent UGV mission failure due to unexpected power exhaustion. Two prediction approaches based on the availability of mission prior knowledge were proposed. The first approach, based on RLS estimation, only uses online power and velocity measurements for energy prediction. The second approach, based on Bayesian estimation, takes advantage of available mission prior knowledge, as well as real-time

measurements, for improving energy predictions. Our comparative experimental and simulation results show that the Bayesian approach can yield more accurate predictions than the RLS approach even in the case of moderately imprecise mission prior knowledge. The results also show that the use of prior knowledge can reduce the false detection and misdetection of abrupt changes in UGV energy consumption. Also, the imprecise mission prior knowledge can be corrected when the similarities among road segments in a mission can be employed using in-advance updating strategies before actual measurements become available.

Future research will focus on how the proposed Bayesian prediction approach can be used for dynamic decision making in a mission. Based on predictions, if the probability of successfully completing the mission is below a desirable threshold, the operator can (a) return to base without completing the mission objectives, (b) revise the initial plan to accomplish fewer objectives before returning (c), perform a recharge and then continue the mission tasks (Wei et al. 2012) or (d) reduce power consumption by turning off sensors and equipment (Mei et al. 2005). If the mission objective cannot change, or if the probability of failure is low, the proposed Bayesian prediction model can be used to dynamically identify optimal paths, among alternatives, with the lowest energy requirements using a stochastic shortest path problem approach. We are currently investigating a heuristic approach that considers the Bayesian prediction uncertainty and its reduction by real-time measurements for dynamic path planning in a network. Another interesting direction is to extend and adapt the Bayesian approach to scenarios in which the UGV traverses environments that are less structured and more difficult to characterize, e.g., a forest floor or earthquake-affected areas.

ACKNOWLEDGMENTS

This research was supported in part by the Ground Robotics Reliability Center (GRRC) at the University of Michigan, with funding from government contract DoD-DoA W56H2V-04-2-0001 through the U.S. Army Tank Automotive Research, Development and Engineering Center (TARDEC).

APPENDIX A

1. Velocity Prediction

The velocity is predicted using an exponentially smoothing model as follows: $E[u(k+1)|u(1:k)] = \hat{u}(k+1|k) = \lambda_u u(k) + (1-\lambda_u)\hat{u}(k|k-1)$, where $u(1:k)$ is the vector of velocity measurements 1 to k, whose initial value is obtained from the prior information of driving style, and λ_u is the EWMA weight. It follows that at measurement k, $\hat{u}(k+j|k) = \hat{u}(k+1|k), \forall j \geq 1$. The variance of prediction error, i.e., $\text{var}\,(u(k+j)|u(1:k))$, is $\sigma_w^2 \sum_{i=1}^{j-1} G_i^2$ where σ_w^2 is the variance, and $G_i = \begin{cases} 1 & \text{for } i = 0 \\ \lambda_u & \text{for } i \geq 1 \end{cases}$ is the Green's function of the underlying EWMA model (Pandit and Wu, 1983).

2. Energy Prediction with the Linear Regression Model (RLS approach)

Let $\hat{\boldsymbol{\beta}}(k) = [\hat{b}(k)\ \hat{C}(k)]^T$ be the estimated parameters at k. $\hat{y}(k+j|k) = E[y(k+j|k)] = E[y(k+j)|x(1:k), \hat{\boldsymbol{\beta}}(k)]$ is the j-step-ahead prediction of response. Additionally, $\hat{P}(k+j|k) = E[p(k+j)|x(1:k), \hat{\boldsymbol{\beta}}(k)]$ is the j-step-ahead prediction of power. $\hat{x}(k+j|k) = W\hat{u}(k+j|k)$ is the j-step-ahead prediction of predictor, and we assume $\hat{y}(k+j|k) \approx \hat{P}(k+j|k)$. The prediction mean is calculated as follows:

$$\begin{aligned} E[y(k+j|k)] &= E[E[y(k+j|k, x(k+j))]] \\ &= \hat{b}(k) + \hat{C}(k)E[x(k+j|k)] \\ &= \hat{b}(k) + \hat{C}(k)\hat{x}(k+j|k). \end{aligned} \tag{A1}$$

The variance of prediction error at k is calculated as follows:

$$\begin{aligned} \text{var}[y(k+j|k)] &= E[\text{var}[y(k+j|k, x(k+j))]] \\ &\quad + \text{var}[E[y(k+j|k, x(k+j))]] \\ &= \sigma_\varepsilon^2 + \hat{C}^2(k)\sigma_w^2 W^2(1 + (j-1)\lambda_u^2). \end{aligned} \tag{A2}$$

The covariance of prediction error at k is calculated as follows:

$$\begin{aligned} &\text{cov}[y(k+j|k), y(k+i|k)] \\ &= E[\text{cov}[y(k+j|k, x(k+j)), y(k+i|k, x(k+i))]] \\ &\quad + \text{cov}[E[y(k+j|k, x(k+j)), E[y(k+i|k, x(k+i))] \\ &= \begin{cases} \hat{C}^2(k)\sigma_w^2 W^2(1 + (j-1)\lambda_u^2) + \sigma_\varepsilon^2 & \text{if } i = j \\ \hat{C}^2(k)\sigma_w^2 W^2(\lambda_u + \min\{i-1, j-1\}\lambda_u^2) & \text{if } i \neq j \end{cases}. \end{aligned} \tag{A3}$$

The variance of the end of mission energy prediction at k is computed as follows:

$$\begin{aligned} \text{var}(\hat{E}_m(k)) &= \text{var}\left(\sum_{j=1}^{\hat{n}-k} y(k+j|k)\right)\Delta t^2 \\ &= \left(\sum_{j=1}^{\hat{n}-k} \text{var}(y(k+j|k)) \right. \\ &\quad \left. + \sum_{i=1}^{\hat{n}-k}\sum_{j\neq i} \text{cov}(y(k+j|k), y(k+i|k))\right)\Delta t^2. \end{aligned} \tag{A4}$$

3. Energy Prediction with the Bayesian Regression Model

The predictive distribution is obtained by computing the integration below:

$$\pi(y(k+j|k)) = \int \pi(y(k+j|k, x(k+j))) \times \pi\,(x(k+j|k))\,dx(k+j), \qquad \text{(A5)}$$

where $x(k+j|k) \sim N(\hat{x}(k+j|k), W^2\sigma_w^2(G_0^2 + G_1^2 + \cdots + G_{j-1}^2))$.

For a mission with two road segments, when $k \le \hat{n}_1$ the integration results in

$$y(k+j|k) \sim \begin{cases} N(\hat{\mu}_b(k|k-1) + \hat{\mu}_{C_1}(k|k-1)\hat{x}(k+j|k), \\ \quad \hat{\mu}_{C_1}^2(k|k-1)W^2\sigma_w^2(G_0^2 + \cdots + G_{j-1}^2) + \sigma_\varepsilon^2) \\ \quad \text{if } j \le \hat{n}_1 - k \\ N(\hat{\mu}_b(k|k-1) + \mu_{C_2}^0\hat{x}(k+j|k), \quad (\mu_{C_2}^0)^2W^2\sigma_w^2 \\ \quad (G_0^2 + \cdots + G_{j-1}^2) + \sigma_\varepsilon^2) \text{ if } j > \hat{n}_1 - k \end{cases}. \qquad \text{(A6)}$$

When $k > n_1$ the integration results in

$$y(k+j|k) \sim N(\hat{\mu}_b(k|k-1) + \hat{\mu}_{C_2}(k|n_1+1:k)\hat{x}(k+j|k), \\ \hat{\mu}_{C_2}^2(k|n_1+1:k)W^2\sigma_w^2(G_0^2 + \cdots + G_{j-1}^2) + \sigma_\varepsilon^2). \qquad \text{(A7)}$$

The covariance of predictions is computed as follows:

$$\begin{aligned} &\operatorname{cov}(y(k+j|k), y(k+i|k)) \\ &\quad = E[\operatorname{cov}[y(k+j|k, x(k+j)), y(k+i|k, x(k+i))]] \\ &\qquad + \operatorname{cov}[E[y(k+j|k, x(k+j))], E[y(k+i|k, x(k+i))]] \end{aligned} \qquad \text{(A8)}$$

$$\text{if } k \le \hat{n}_1 \begin{cases} \hat{\mu}_{C_1}^2(k|k-1)\sigma_w^2W^2(\lambda_u + \min\{i-1, j-1\}\lambda_u^2) \\ \quad \text{if } i, j \le \hat{n}_1 - k \text{ and } j \ne i \\ \sigma_\varepsilon^2 + \hat{\mu}_{C_1}^2(k|k-1)\sigma_w^2W^2(1 + (j-1)\lambda_u^2) \\ \quad \text{if } i, j \le \hat{n}_1 - k \text{ and } j = i \\ \hat{\mu}_{C_1}(k|k-1)\mu_{C_2}^0\sigma_w^2W^2(\lambda_u + \min\{i-1, \\ \quad j-1\}\lambda_u^2) \text{if } i \le \hat{n}_1 - k,\ i > \hat{n}_1 - k \\ \quad \text{or if } i > \hat{n}_1 - k,\ i \le \hat{n}_1 - k \\ (\mu_{C_2}^0)^2\sigma_w^2W^2(\lambda_u + \min\{i-1, j-1\}\lambda_u^2) \\ \quad \text{if } i, j > \hat{n}_1 - k \text{ and } j \ne i \\ \sigma_\varepsilon^2 + (\mu_{C_2}^0)^2\sigma_w^2W^2(1 + (j-1)\lambda_u^2) \\ \quad \text{if } i, j > \hat{n}_1 - k \text{ and } j = i \end{cases}$$

$$\text{if } k > n_1 \begin{cases} \hat{\mu}_{C_2}^2(k|n_1+1:k) \\ \sigma_w^2W^2(\lambda_u + \min\{i-1, j-1\}\lambda_u^2) \text{ if } j \ne i \\ \sigma_\varepsilon^2 + \hat{\mu}_{C_2}^2(k|n_1+1:k)\sigma_w^2W^2(1 + (j-1)\lambda_u^2) \\ \text{if } j = i. \end{cases}$$

The variance of prediction for missions that are composed of more than two road segments is a straightforward extension of the presented equations. The variance of mission energy prediction can be computed in a similar way as was discussed in the case of regression.

4. Energy Prediction Confidence Interval

The confidence intervals of energy prediction for both models are computed using $E[\hat{E}_m] \pm z_{1-\alpha}\sqrt{\operatorname{var}(\hat{E}_m)}$. We have assumed that $\sum_{j=1}^{\hat{n}-k} y(k+j|k)$ is approximately normal.

REFERENCES

Carlson, J., & Murphy, R. (2003). Reliability analysis of mobile robot. IEEE International Conference on Robotics and Automation (ICRA), Taipei, Taiwan (vol. 1, pp. 274–281).

Carlson, J., & Murphy, R. (2005). How UGVs physically fail in the field. IEEE Transactions on Robotics, 21(3), 423–437.

Carlson, J., Murphy, R., & Nelson, A. (2004). Follow-up analysis of mobile robot failures. IEEE International Conference on Robotics and Automation (ICRA), New Orleans (pp. 4987–4994).

Ceraolo, M., & Pede, G. (2001). Techniques for estimating the residual range of an electric vehicle. IEEE Transactions on Vehicular Technology, 50(1), 109–115.

Congdon, P. (2003). Bayesian statistical modelling. Chichester, England, John Wiley & Sons, Ltd.

Dressler, F., & Fuchs, G. (2005). Energy-aware operation and task allocation of autonomous robots. Proceedings of the Fifth IEEE International Workshop on Robot Motion and Control, Dymaczewo, Poland (pp. 163–168).

Gondor, J., Markel, T., Simpson, A., & Thornton, M. (2007). Using global positioning system travel data to assess real-world energy use of plug-in hybrid electric vehicles. Transportation Research Record, (2017), 26–32.

Gorjian, N., Ma, L., Mittinty, M., Yarlaqadda, P., & Sun, Y. (2009). A review on degradation models in reliability analysis. Proceedings of the 4th World Congress on Engineering Asset Management, Athens: Springer.

Kramer, J., & Murphy, R. (2006). Endurance testing for safety, security and rescue robots. Performance Metrics for Intelligent Systems (PERMIS) (pp. 247–254).

Ljung, L. (1999). System identification: Theory for the user. Upper Saddle River, NJ: Prentice-Hall.

Lu, H., Kolarik, W. J., & Lu, S. (2001). Real-time performance reliability prediction. IEEE Transactions on Reliability, 50(4), 353–357.

Lu, S., Lu, H., & Kolarik, W. J. (2001). Multivariate performance reliability prediction in real-time. Reliability Engineering and System Safety, 72(1), 39–45.

Mei, Y., Lu, Y., Hu, Y., & Lee, C. (2004). Energy-efficient motion planning for mobile robots. IEEE International Conference on Robotics and Automation (ICRA), New Orleans (vol. 5, pp. 4344–4349).

Mei, Y., Lu, Y., Hu, Y., & Lee, C. (2005). A case study of mobile robot's energy consumption and conservation techniques. IEEE International Conference on Advanced Robotics, Seattle (pp. 492–497).

Montgomery, D. (2005). Introduction to statistical quality control, 5th ed. Hoboken, NJ: John Wiley & Sons, Inc.

Pandit, S. M., & Wu, S. M. (1983). Time Series and system analysis with applications. New York: John Wiley & Sons, Inc.

Proffitt, D. R., Bhalla, M., Gossweiler, R., & Midgett, J. (1995). Perceiving geographical slant. Psychonomic Bulletin & Review, 2(4), 409–428.

Sadrpour, A., Jin, J., Ulsoy, A. G., & Lee, H. J. (2011). Simulation-based acceptance testing for unmanned ground vehicles. International Journal of Vehicle Autonomous Systems (in press).

Sadrpour, A., Jin, J., & Ulsoy, A. G. (2012). Mission energy prediction for unmanned ground vehicles. IEEE International Conference on Robotics and Automation (ICRA), St. Paul, MN.

Sadrpour, A., Jin, J., & Ulsoy, A. G. (2013). Experimental validation of mission energy prediction model for unmanned ground vehicles. ASME American Control Conference (ACC), Washington, DC.

Saha, B., & Goebel, K. (2008). Uncertainty management for diagnostics and prognostics of batteries using Bayesian techniques. IEEE Aerospace Conference, Big Sky, MT (pp. 1–8).

Saha, B., Poll, S., Goebel, K., & Christophersen, J. (2007). An integrated approach to battery health monitoring using Bayesian regression and state estimation. IEEE Autotestcon Conference, Baltimore (pp. 646–653).

Saha, B., Goebel, K., & Christophersen, J. (2009). Comparison of prognostic algorithms for estimating remaining useful life of batteries. Transactions of the Institute of Measurement and Control, 31(3–4), 293–308.

Saha, B., Koshimoto, E., Quach, C., Hogge, E., Storm, T., Hill, B., Vazquez, S., & Goebel, K. (2011). Battery health management system for electric UAVs. IEEE Aerospace Conference, Big Sky, MT (pp. 1–9).

Stancliff, S., & Dolan, J. (2005). Towards a predictive model of mobile robot reliability. Technical report, Pittsburgh, PA.

Tilbury, D. M., & Ulsoy, A. G. (2011). A new breed of robots that drive themselves. ASME Mechanical Engineering Magazine, 133, 28–33.

Ulsoy, A., Peng, H., & Cakmakci, M. (2012). Automotive Control Systems. Cambridge University Press.

Vichare, N., Rodgers, P., Eveloy, V., & Pecht, M. (2007). Environment and usage monitoring of electronic products for health assessment and product design. Quality Technology & Quantitative Management, 4, 235–250.

Wei, H., Wang, B., Wang, Y., Shao, Z., & Chan, K. C. C. (2012). Staying-alive path planning with energy optimization for mobile robots. Expert Systems Applications, 39(3), 3559–3571.

Wong, J. Y. (2008). Theory of Ground Vehicles. Hoboken, NJ: John Wiley & Sons, Inc.